

# Impact of climate change on energy use and bioclimatic design of residential buildings in the 21st century in Argentina



Silvana Flores-Larsen <sup>a,\*</sup>, Celina Filippín <sup>b</sup>, Gustavo Barea <sup>c</sup>

<sup>a</sup> Instituto de Investigaciones en Energía No Convencional (INENCO) - Universidad Nacional de Salta – CONICET, Avenida Bolivia 5150, Salta 4400, Argentina

<sup>b</sup> CONICET, CC302 Santa Rosa, La Pampa 6300, Argentina

<sup>c</sup> Instituto de Ambiente, Hábitat y Energía (INAHE) – CONICET, Av. Ruiz Leal s/n Parque General San Martín, Mendoza 5500, Argentina

## ARTICLE INFO

### Article history:

Received 5 November 2018

Revised 13 December 2018

Accepted 14 December 2018

Available online 21 December 2018

### Keywords:

Heating and cooling energy consumption

Future climate

Thermal simulation of buildings

## ABSTRACT

Climate change will have great impacts on building's energy consumption and design of future buildings should consider this situation. The aims of this research are to evaluate the impact of climate change on the energy performance of residential buildings and to analyze if bioclimatic strategies that are appropriate for present climatic conditions should be applied in the design of future buildings. A compact conventional housing that represents an Argentinean typical mid-income house was simulated with EnergyPlus software and calibrated with measured data. Energy consumption and bioclimatic strategies were analyzed for future data under A2 scenario. The change of annual energy use between the baseline period (1961–1990) and 2080 is predicted to range from –25% to 8% for conventional housing buildings. The energy destined to air heating and cooling will be 23%–59% lower and 360–790% higher, respectively, in 2080 than in the baseline period (1961–1990). These values correspond to decreases between 6.0 and 7.6 kWh/m<sup>2</sup>·decade (heating) and increases between 1.7 and 8.4 kWh/m<sup>2</sup>·decade (cooling). Recommendations on future building design and building retrofit are done. Sunshading together with a reduction of direct solar gains and natural ventilation were found to be the most effective design strategies to counteract climate changes in future buildings.

© 2018 Elsevier B.V. All rights reserved.

## 1. Introduction

Buildings consume about 40% of the overall energy consumption worldwide and they are also responsible for carbon emissions. Greenhouse gas emissions (GHG) from the building sector have more than doubled since 1970 [1]. Despite efforts to reduce emissions to the atmosphere, clearly documented by the Intergovernmental Panel on Climate Change (IPCC) the global climate is undergoing a consistent and inevitable change and the problem of climate change is drawing attention from the academia worldwide. The level of GHG in different scenarios projected by IPCC demonstrated dramatic rise in the coming future [2]. The energy use and related emissions are expected to double –or potentially even triple– by mid-century due to several key trends. This dangerous trend could be partially reverted if today's cost-effective best practices and technologies are broadly diffused; the final energy use could stay constant or even decline by mid-century, as com-

pared to today's levels [3]. In this context, buildings represent a critical piece of a low-carbon future and a global challenge for integration with sustainable development [4].

At world level, the latest report from the World Meteorological Organization [5] confirms that 2016 was the warmest year of all recorded ones: there was a surprising increase of 1.1 °C above pre-industrial levels and 0.06 °C with respect to the previous record of 2015. As GHG concentrations continue to rise, we expect to see future changes to the climate system that are greater than those already observed and attributed to human activities. In South America, temperatures will increase in the future, with greatest warming projected in southern Amazonia. Also the frequency of warm nights will increase together with a decrease in the frequency of cold nights [6]. In Argentina, the comparison between 1961 and 2016 (Fig. 1) indicates that the annual mean temperatures increased throughout the country between 0.3 °C and 2 °C (West Patagonia). The exception is the central zone, where the annual mean temperature remained constant, probably due to higher cloudiness and precipitation levels. In summer, the mean maximum temperature (December to February) increased between 0.3 °C and 2 °C were observed, excepting the central zone where decreases between –0.3 and –1 °C were found. In winter (June to

\* Corresponding author.

E-mail addresses: [seflores@unsa.edu.ar](mailto:seflores@unsa.edu.ar) (S. Flores-Larsen), [cfilippin@cepenet.com.ar](mailto:cfilippin@cepenet.com.ar) (C. Filippín), [gbarea@mendoza-conicet.gov.ar](mailto:gbarea@mendoza-conicet.gov.ar) (G. Barea).

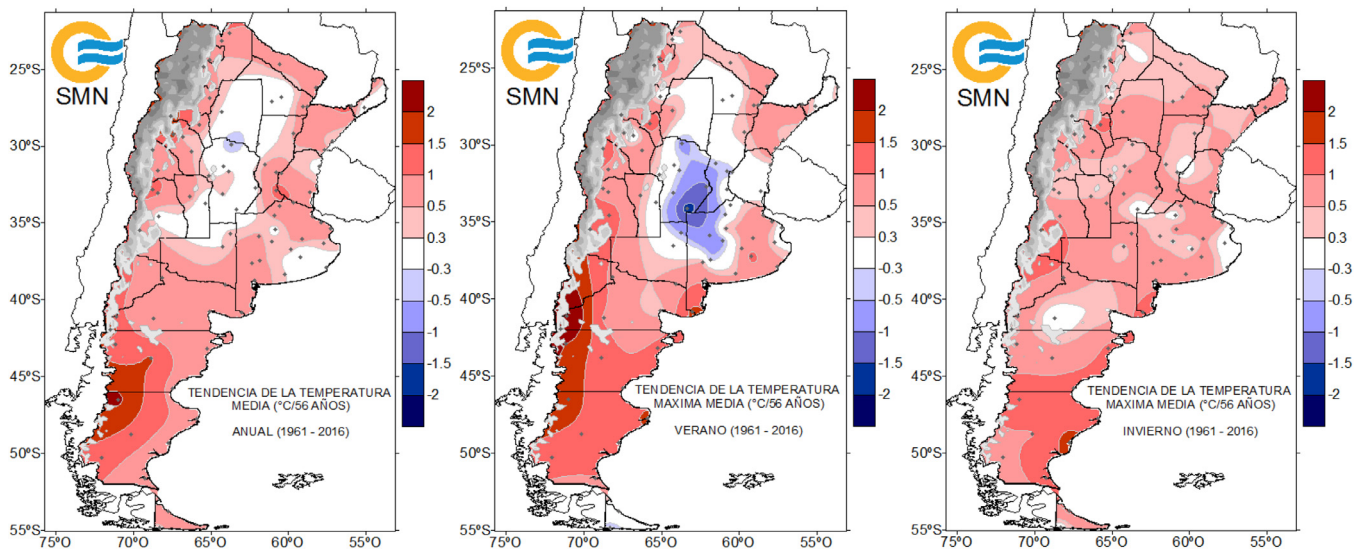


**Fig. 1.** Temperature differences ( $^{\circ}\text{C}/56$  years) in annual mean temperature (left), average maximum in summer (center), and average maximum in winter (right) in Argentina, for 2016 versus 1961. Source: National Meteorological Service [8].

August), average maximum temperature also increased, between  $0.5^{\circ}\text{C}$  and  $1^{\circ}\text{C}$ . The most affected regions were Patagonia, the Andean region and Littoral (Northeast) region. Furthermore, future projections for Argentina of the regional climate model MM5 version 3.6, developed by Penn State University and the National Centers for Environmental Prediction/National Centre for Atmospheric Research indicate that the observed tendencies described below will deepen in the future [7]. Projections by the end of the 21st century (A2 emission scenario) show both an increase of mean temperature ranging from  $1.5$  to  $5.5^{\circ}\text{C}$  (depending on the season and region, with the highest increases over subtropical latitudes), and an increase of precipitation in central Argentina. This regional model also projects a maximum temperature increase (between  $4$  and  $5^{\circ}\text{C}$ ) over subtropical latitudes mainly during spring.

In urban areas, the increase of the air temperatures due to the global warming is also enhanced by the heat island phenomenon, and these high temperatures intensify the energy demand in cities, deteriorate urban comfort conditions, endanger the vulnerable population and amplify pollution problems especially in regions with hot climates. Kapsomenakis et al. [9] analyzed 40 years of hourly data series from nine meteorological stations in Greece and concluded that, for a typical office building, the heating load decreased by about  $1\text{ kWh}/\text{m}^2$  per decade and the cooling load increased by about  $5\text{ kWh}/\text{m}^2$  per decade. This phenomenon has major environmental, economic and social consequences, which will be amplified in the upcoming decades in view of the expected man-made climatic changes in this geographic area. Asimakopoulos et al. [10] showed that the energy demand for heating the building sector in Greece could decrease by about 90%, while the respective energy demand for cooling could increase by as much as 248% until 2100 (scenario A2). Andric et al. [11] concluded that, in heating dominant climates of developed countries, heat demand could decrease in the future due to the application of building renovation policies. Kolokotroni et al. [12] studied the energy consumption of office buildings in London in the mid-future year 2050. The predictions confirm that heating load decreases, cooling load and overheating hours increase from present to future years. It is shown that night cooling using natural ventilation will have beneficial effects. A lot of research was conducted for USA climates. Shen [2] describes different case studies in four representative cities in the USA and shows that climate change will have great impacts on residential and office building energy

use in the period 2040–2069. The change of annual energy use is predicted to range from  $-1.64\%$  to  $14.07\%$  for residential buildings and from  $-3.27\%$  to  $-0.12\%$  for office buildings under A2 scenario. The results suggest that the climate change will narrow the gap of energy use for residential buildings located in cold and hot climate regions in USA and it generally will reduce office building energy use in the future. It is also found that the growing peak electricity load during cooling seasons will exert a greater pressure for the future grid. Similar results were found by Wang and Chen [13], who studies the changes in energy use for building heating and cooling in USA. They conclude that there would be a net increase in source energy use in heating and cooling by the 2080s for hot humid, warm humid, and mixed humid climate zones and a net decrease in cold and very cold climate zones based on the HadCM3 weather projection for three scenarios (A1F1: high emission; A2: medium emission, and B1: low emission). Wang et al. [14] studied the impact of climate change on the energy consumption of a medium-size office building located in five different cities, in USA, by using EnergyPlus software and future climate models HadCM3 and CESM1. They found that the overall impact of climate change on energy consumption varied with climate zones, with substantial increases in building energy use in Miami, Phoenix, and Los Angeles. The authors studied different mitigation measures related to HVAC operation and found that the mixed-mode ventilation measure was the most effective to counteract climate changes. In Argentina, studies about the impact of climate change on building's energy consumption are nowadays in their initial steps. Filippín et al. [15], studied the energy consumption of 10 single-family dwellings in the central region of Argentina for a period of 50 years together with different retrofitting strategies for future weather conditions in 2039. The CMIP5-Coupled Model Intercomparison Project-Phase 5 (RCP 4.5) was used. The results indicate that the addition of thermal insulation in walls and roofs is highly beneficial, but the increase of glazed areas seems to be counterproductive. The energy demands for 2010 and 2039, for both the conventional and the retrofitted dwelling, show a decrease (22%) in winter and an increase of (about five times) in summer. It is concluded that some design suggestions applied in the present (i.e., the glazed to floor area relationship) should be revised. Thus, buildings designed today must satisfy the architectonic and functional requirements of the present time, and also they must consider the weather data for the future due to the climate change.

As shown, scientists across the world are making efforts to develop several strategies to reduce the building's energy consumption. Different mitigation and adaptation techniques can be proposed for the building sector, depending on the future scenarios. In particular, the development and use of passive and advanced cooling techniques for buildings offer very significant possibilities to improve the energy performance of buildings during the summer period [16,17,12]. But, in a changing climate, some passive strategies and retrofit actions that could be enough good at present, could not be so good in the future (i.e., they could cause overheating in summer). Thus, while bioclimatic strategies are nowadays well known and spread, a new vision about its efficiency under future climatic conditions should be faced. This challenge needs to be studied at regional levels, due to the also regional characteristics of future climate changes. In this context, the two aims of the present research are evaluating the impact of climate change on the energy performance of a compact conventional housing with the typical construction of an Argentinean mid-income house, and analyzing if bioclimatic strategies appropriate for present climatic conditions should be applied in the design of future buildings. A set of four sites in different temperate and warm climates of Argentina were selected and the impact on energy consumption of different bioclimatic and passive strategies were analyzed, for medium and long-term climate change (2020, 2050, and 2080). Recommendations on future building design and building retrofit are done.

## 2. Methodology

This study is split into three main parts. The first one describes the building selected as the case study and the validation of its thermal model with measured data. The second part presents the methodology used to select the sites and the generation of future climatic data. The third part discusses the heating and cooling energy consumption of the case-study building for present and future climate. The fourth part compares the applicability of bioclimatic design strategies and retrofit measures in present and future climate conditions and discusses the main results of the study.

### 2.1. Selection of the case-study and thermal modeling

A compact conventional house is selected as case-study, which is representative of the conventional construction of single-family dwellings in Santa Rosa city. Firstly, the house design together with material properties and climate description are provided. Then, a detailed thermal modeling is performed for an annual period in order to obtain the annual energy consumption. The software used to simulate the house is EnergyPlus V8.9 [18], an open-source code published by the U.S. Department of Energy that is widely used in the simulation of building performance. The climatic data input in EnergyPlus is a plain text file in a special format, EPW (Energy-Plus Weather). Thus, the bi-monthly results of energy consumption provided by EnergyPlus are compared and adjusted with the real energy consumption of the house, averaged on a period of 15 years (1996–2011). This process allows obtaining a validated thermal model of the house that can be relocated to other cities of the country and subjected to changes in the climatic data.

### 2.2. Selection of the new sites and generation of future climatic data

A set of representative cities of Argentina is selected, corresponding to the northern, center and Andean regions of the country. The northern region is characterized by hot and humid summers and temperate dry winters, while the center region is characterized by a precipitation with monsoon conditions and a dry (and colder) winter season. The Andean region is conditioned by

the Andes orography, with very arid zones in piedmont and predominantly clear skies. Then, a set of sub-criteria was used to narrow the selection by eliminating locations that did not meet the following two criteria: availability of real climatic data for the period 1961–1990, and accuracy of the software to predict future climate for these locations. In relation to the first criteria, the original selected set of sites was narrowed by eliminating those cities without real data provided by meteorological stations. The selection of cities where measured data is available avoids the necessity of interpolating data between existent stations that can be far away from each other in Argentina. Thus, a resulting sub-set of 8 candidate sites (Table 1 and Fig. 2) was obtained, for which it is possible to generate a typical meteorological year derived from measured data in the site, for the baseline period 1961–1990, by using the software Meteonorm [19]. The selection of 1961–1990 period as base climate is due to the requirements of the software that generates the "future climate", CCWorldWeatherGen [20] that performs the calculations based on climatic data averaged on the mentioned period. Using more recent data could lead to erroneous or overestimations in the future temperature shifts.

This sub-set was narrowed again by considering the second criteria: the capacity of the software to generate meteorological files of future climate for use in building simulation, which is currently a subject of discussion and research [23,24]. The selected software was CCWorldWeatherGen V1.9, a tool widely used in the field of thermal simulation of buildings. This software was developed by the Sustainable Energy Research Group of the University of Southampton [25] for the generation of future data through the method of "morphing". The method uses both, a "present time" weather file based on 1961–1990 averages and the monthly mean predictions of the IPCC HadCM3 GCM global model developed by the Hadley Centre of the United Kingdom, to generate future hourly data for the years 2020, 2050 and 2080. The "present climate" hourly data is loaded into an Excel sheet that provides the interface to the morphing procedure for a medium-high emissions scenario A2. This scenario describes a world with a fast population increase and intense energy consumption. Four points, the nearest and more representative of the selected site, are automatically selected to provide an average of three different ensemble members (A2a, A2b, and A2c, the three are simulated using the same parameters with different initializations and averaged to reduce the noise in the model run). For the case of the locations that we will address in this article, the problem presented by the IPCC HadCM3 model is the coarse resolution of the grid (3.75° longitude x 2.5° latitude, which represents an average grid of 420 km x 280 km). At the regional level, the climate is the result of complex processes that vary strongly with location and so respond differently to the global-scale changes [26]. Thus, a coarser grid force, in some cases, an average of four points that are not representative of the locality, particularly in mountainous areas and valleys where the microclimates are completely different. For example, some cities near the Andes will be calculated in CCWorldWeatherGen by averaging two points to the west of the Andes mountain range and two points to the east, on the Chilean seacoast, which are clearly not adequate. For the sites of the present article, the four points automatically selected by the software (A, B, C and D in Table 1) were checked and, when none of them were representative of the site, it was discarded. Thus, four potential sites were finally obtained: Santa Rosa, Mendoza, Córdoba, and Orán, for which the points to be averaged were manually selected (in bold in Table 1). In the Excel sheet, the non-desired points were overwritten with the data of the manually selected points, previous to the average and calculation procedure. Thus, we generated EPW files for 2020, 2050 and 2080, for the four locations (12 files in total). The selected future years (2050–2080) agree with the concept that an existing building has a useful life of fifty years, according to some revised

**Table 1**

Original set of sites, bio-environmental climates from Argentinean Norm (IRAM 11,603 [21]: IIIa: warm temperate with thermal amplitudes higher than 14 °C, IVa: cold temperate mountainous, IIb: warm with thermal amplitudes lower than 14 °C) and geographic coordinates. The grey cells show the sites where the generation of future data with CCWorldWeatherGen software is not accurate. (\*) HADCM3 grid points used for manual average are presented in bold letter.

Site	Koppen climate classification	Bio-environmental zone (IRAM Norm 11603/96)	Geographic coordinates	Altitude (m)	HADCM3 grid points automatically selected by CCWorldWeatherGen(*)
Santa Rosa	Cfa	IIIa	-36.57°S -64.27°W	191	A: -40.00°S, -63.75°W, 71 m <b>B: -35.00°S, -63.75°W, 142 m</b> <b>C: -37.50°S, -63.75°W, 157 m</b> D: -37.50°S, -67.50°W, 450 m
San Luis	Bsk	IIIa	-33.27°S -66.35°W	713	A: -35.00°S, -67.50°W, 462 m B: -32.50°S, -63.75°W, 300 m C: -32.50°S, -67.50°W, 566 m D: -35.00°S, -63.75°W, 142 m
Mendoza	Bwk	IVa	-32.83°S -68.78°W	704	<b>A: -32.50°S, -67.50°W, 566 m</b> B: -32.50°S, -71.25°W, 750 m C: -30.00°S, -67.50°W, 1240 m D: -35.00°S, -67.50°W, 462 m
Córdoba	Cwa	IIIa	-31.40°S -64.18°W	425	A: -32.50°S, -67.50°W, 502 m B: -30.00°S, -67.50°W, 1016 m <b>C: -30.00°S, -63.75°W, 440 m</b> <b>D: -32.50°S, -63.75°W, 300 m</b>
San Juan	Bwk	IIIa	-31.57°S -68.42°W	598	A: -32.50°S, -71.25°W, 450 m B: -32.50°S, -67.50°W, 502 m C: -30.00°S, -71.25°W, 281 m D: -30.00°S, -67.50°W, 1016 m
Catamarca	Bsh	IIa	-28.60°S -65.67°W	454	A: -27.50°S, -67.50°W, 1940 m B: -27.50°S, -63.75°W, 154 m C: -30.00°S, -63.75°W, 426 m D: -30.00°S, -67.50°W, 1016 m
Salta	Cwb	IIIa	-24.85°S -65.48°W	1221	A: -25.00°S, -67.50°W, 3670 m B: -22.50°S, -67.50°W, 4430 m C: -25.00°S, -63.75°W, 330 m D: -22.50°S, -63.75°W, 433 m
Orán	Cwa	IIb	-23.15°S -64.32°W	357	A: -22.50°S, -67.50°W, 4430 m B: -20.00°S, -63.75°W, 1000 m <b>C: -22.50°S, -63.75°W, 433 m</b> D: -25.00°S, -63.75°W, 330 m

**Table 2**

Historical climatic data (monthly mean temperature, relative humidity, solar irradiance on horizontal surface, annual Heating Degree Days HDD and Cooling Degree Days CDD) of the four sites for the period 1961–1990 (obtained from Meteonorm [19]), and temperature  $T_n$  of thermal neutrality calculated from ASHRAE 55–17 [29] ( $T_n = 17.8 + 0.31 * T_m$ ,  $10^\circ C < T_m < 33.5^\circ C$ ) and from Pérez-Fargallo et al. [30] ( $T_n = 13.6^\circ C + 0.678T_m$ ,  $6.5^\circ C < T_m < 10^\circ C$ ).

Site	Mean temperature $T_m$ (°C)		Mean relative humidity (%)		Annual HDD (baseline 18 °C)	Annual CDD (baseline 18 °C)	Mean solar irradiance on a horizontal surface (Wh/m <sup>2</sup> )		Thermal neutrality $T_n = 17.8 + 0.31 * T_m$	
	July	January	July	January			July	January	July	January
Santa Rosa	7.5	23.9	76	55	1538	593	2179	5785	18.7	25.2
Mendoza	7.7	25.2	66	48	1349	842	2564	7029	18.7	25.6
Córdoba	11.1	24.2	64	63	861	828	2400	6764	21.2	25.3
Orán	14.4	26.1	82	77	412	1518	2399	5997	22.3	25.9

literature on carbon emission research of the building's life cycle [27,28].

**Table 2** shows the historical climatic data (monthly mean temperature, relative humidity, solar irradiance on a horizontal surface, annual Heating Degree Days HDD and Cooling Degree Days CDD) of the four sites for the period 1961–1990 (obtained from Meteonorm), and the temperatures of thermal neutrality. These values were calculated either, with ASHRAE 55–17 [29] when mean outdoor temperatures falls between 10 °C and 33.5 °C, or with the model of Pérez-Fargallo et al. [30] for mean outdoor temperatures between 6.5 °C and 10 °C.

### 2.3. Simulation of the energy consumption of the case-study building for future climate and analysis of design strategies in present and future climatic conditions

To simulate the energy consumption of the case-study building, the previously obtained EnergyPlus model is used under future weather conditions generated by the CCWorldWeatherGen tool. A comparative analysis of the heating and cooling energy consumption for the four selected sites is performed, for the baseline period (1961–1990) and for the future weather (2020, 2050, and 2080).

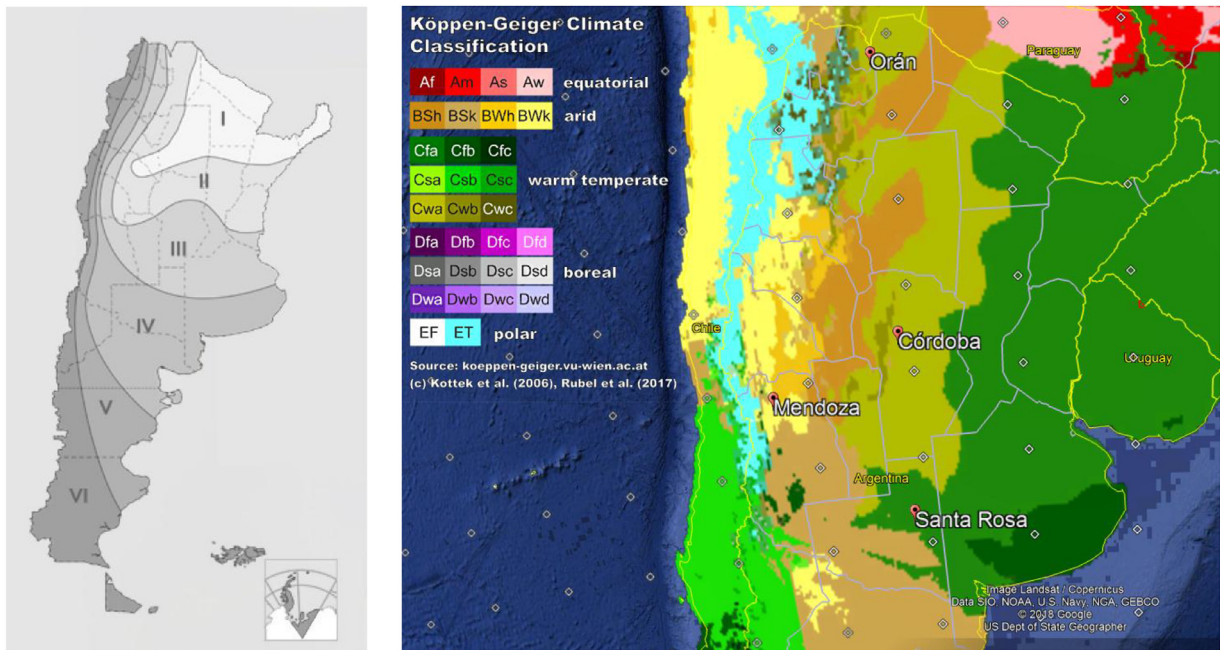


**Fig. 2.** Argentinean bioclimatic regions (IRAM Norm 11,603 [21]) (left) and view in Google Earth of the Koppen climate classification [22] (right) together with HADCM3 grid points and the final set of cities used in this study.

The efficiency of different passive heating and cooling strategies for a given climate is analyzed by using the bioclimatic chart. This chart allows detecting and ordering the available bioclimatic strategies in view of their efficiencies for a given climate. In particular, ClimateConsultant V6.0 [31] was used. This software reads a climatic file in EPW format and translates the climatic information into different graphics and into the psychrometric chart, where 16 different Design Strategy Zones gives a relative idea of the most effective passive heating or passive cooling strategies. Climate Consultant analyses the distribution of this psychrometric data in each Design Strategy zone in order to create a unique list of Design Guidelines for a particular location. This tool was used in this study to analyze the most effective strategies for the baseline period (1961–1990) and for the future climatic conditions.

### 3. Description of the case study and thermal model

The case study is located in Santa Rosa city, capital of La Pampa province in central Argentina ( $36^{\circ}27' S$ ,  $64^{\circ}27' W$ , 182 m o.s.l.). The climate is classified as cold temperate zone IIIa (IRAM Norm 11,603 [21]) and Cfa from Koppen-Geiger classification. It is a compact conventional house between party walls. Its design and construction materials are typical of the '60s. The useful area is  $50 \text{ m}^2$  and the house volume is  $140 \text{ m}^3$  (Fig. 3), with a glazed area to North of about 4.8% of the useful area. The construction layout, thermal transmittances and material properties of each layer in walls, floors, and roofs are shown in Table 3. The exterior envelope and the interior walls do not include thermal insulation, as usual in Argentina. The Global Heat Loss Coefficient is  $G = 3.00 \text{ W m}^{-3} \text{ K}^{-1}$ , which is higher than the admissible value of  $1.88 \text{ W m}^{-3} \text{ K}^{-1}$  required by the non-compulsory Argentinean Norms (IRAM 11,604 [32]). The same Norm estimates an annual heating load of about  $290 \text{ kWh/m}^2$  for this house.

In a previous research work [33], the historical energy consumption of this house, between 1996 and 2011, was studied. The average annual consumption of electricity was  $21.3 \text{ kWh/m}^2$ , while the average annual consumption of natural gas was  $432 \text{ kWh/m}^2$  with low variability (variability coefficients between 6% and 10%).

Thus, the space heating energy is estimated in  $290 \text{ kWh/m}^2$  (considering a 67% of the annual gas consumption destined to space heating, as estimated by the statistics gas company in the region), a value that approximates the annual heating load previously estimated by IRAM Norm 11,604 considering a thermal efficiency of 0.65 for the gas heaters [34].

### 3.2. Thermal simulation and validation of the building model

The house was simulated with EnergyPlus V8.9 software and the results of the simulated bi-monthly energy consumption were compared with the real bi-monthly historical data. Because the details of the model validation are given in [33], here we reproduce only the main aspects of the model. The thermal properties and thicknesses of the construction layers of walls, roofs, and floors are those shown in Table 3. The house was divided into 6 thermal zones, whose floor areas, volumes and internal heat gains are shown in Table 4. The interior heat gains due to people are described by the occupancy and activity level schedules (sleeping: 40 W, cooking: 100 W; reading: 80 W). The air renewals due to infiltrations were estimated by considering the total frame' length, air infiltration for normal carpentry of wood frames (IRAM 11,507–2001 [35]), a correction factor of the external environment and wind velocity. The infiltration rate was estimated in  $2.8 \text{ m}^3/\text{h}$  for the Bedrooms and Livingroom. The total air renewals were estimated in 3 ach/hour [36].

Natural ventilation is allowed when the exterior conditions are good enough. The HVAC cooling system is turned on when indoor conditions are out of the adaptive comfort zone (ASHRAE Standard 55). A 65% efficiency was considered for the air conditioning system. For comfort calculations, 1clo and mean indoor velocity of  $0.5 \text{ m/s}$  were used.

The bi-monthly energy consumption for air heating simulated with EnergyPlus was compared with the bi-monthly historical data in order to adjust the model. The total annual energy consumption simulated with EnergyPlus for air heating was  $289.5 \text{ kWh/m}^2$ , while the historical consumption of natural gas for heating was  $290 \text{ kWh/m}^2$ . For this house, 97% of the energy is destined to air

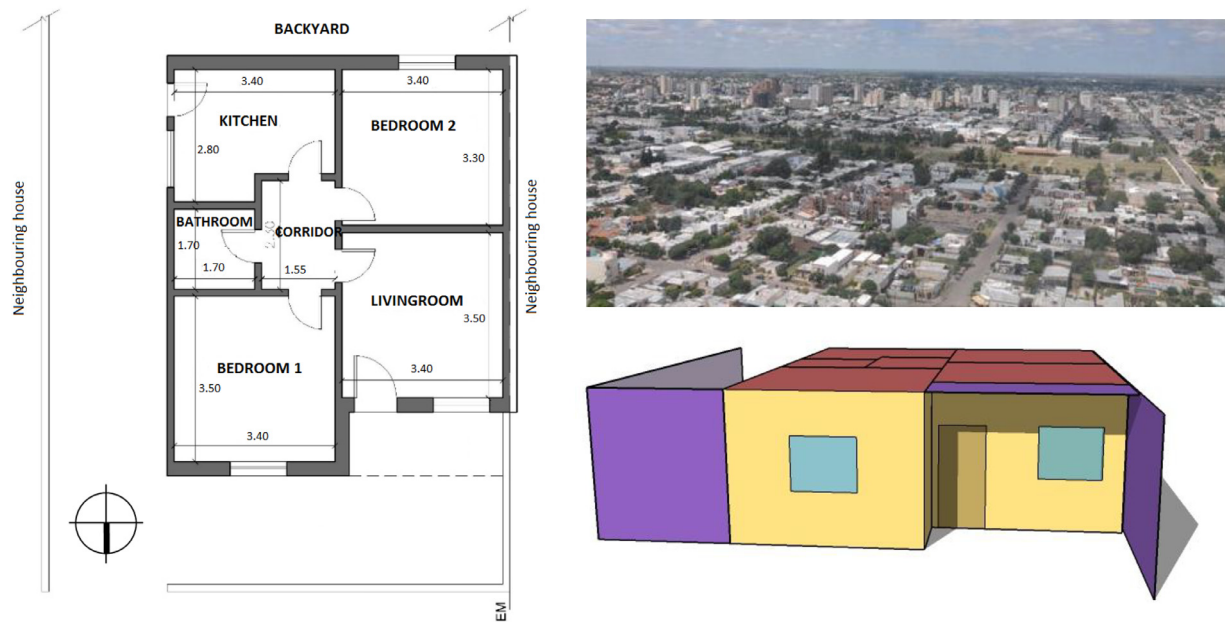


**Fig. 3.** Plan view (left), SketchUp model of the house designed for EnergyPlus and urban environment in Santa Rosa (right).

**Table 3**

Construction materials of the envelope elements of the studied house.

	Layers (from outdoor)	Finishing painting/color	Thermal transmittance K (W/m <sup>2</sup> K)	IRAM Norm 11,604 compliance
Exterior walls	Plaster (0.02 m) Massive ceramic brick (0.30 m) Plaster (0.02 m)	Beige (exterior) White (interior)	2.04	Level C (K = 2) not reached
Interior walls	Plaster (0.02 m) Massive ceramic brick (0.15 m) Plaster (0.02 m)	White (both sides)	2.97	–
Roof	Forged pre-stressed concrete beams, ceramic blocks and concrete compression layer with a waterproof membrane.	Beige	2.03	Level C (K = 1) not reached
Windows	Simple glazing Clear glass 4mm	Not applicable	2.79 (shutters closed) 5.1 (shutters open)	–
Doors	Wood carpentry with wood shutters Wood layer (interior: 35 mm thick; exterior: 45 mm thick)	Brown	3.1	–

**Table 4**

Internal heat gains due to people and electric appliances included in the thermal simulation.

Thermal zone	Floor area (m <sup>2</sup> )	Internal heat gains		
		Volume (m <sup>3</sup> )	Electric appliances (W)	People (W)
Bedroom 1	13.2	37.1	69	80
Living	13.5	37.9	69	320
Corridor	4.2	11.7	23	0
Bathroom	3.4	9.6	46	0
Kitchen	9.7	27.2	196	400
Bedroom 2	12.8	35.8	23	80

heating and 3% to air cooling. The seasonality of the energy consumption is strong, with higher values in winter (details in [33]).

#### 4. Results

##### 4.1. Results of 'morphing' for 2020, 2050 and 2080

Table 5 shows the results of the morphing procedure with CC-worldWeatherGen. Annual averages resulting in the four selected cities are shown, for the baseline period 1961–1990 and for the years 2020, 2050 and 2080. It is concluded that, in all sites, the air temperature will increase in the future, with higher increases in cities with lower latitudes. For example, between 2020 and 2080

the air temperature will rise 2.2 °C, 2.7 °C, 2.8 °C, and 3.8 °C in Santa Rosa, Mendoza, Córdoba, and Orán, respectively (annual average). These results are in line with findings of regional climate models for Argentina that predict higher increases in the north of the country [37]. The changes in annual solar irradiance and wind speed for the four cities are very small when compared with the baseline TMY. Also, the changes in relative humidity are not very significant at annual averages.

Figs. 4–6 show the monthly temperature differences for air mean, maximum and minimum temperatures for the four cities, calculated as differences between 2080 and the baseline period 1961–1990. In all sites, the highest increases will occur in spring and summer. Orán is the site with the highest increases: between

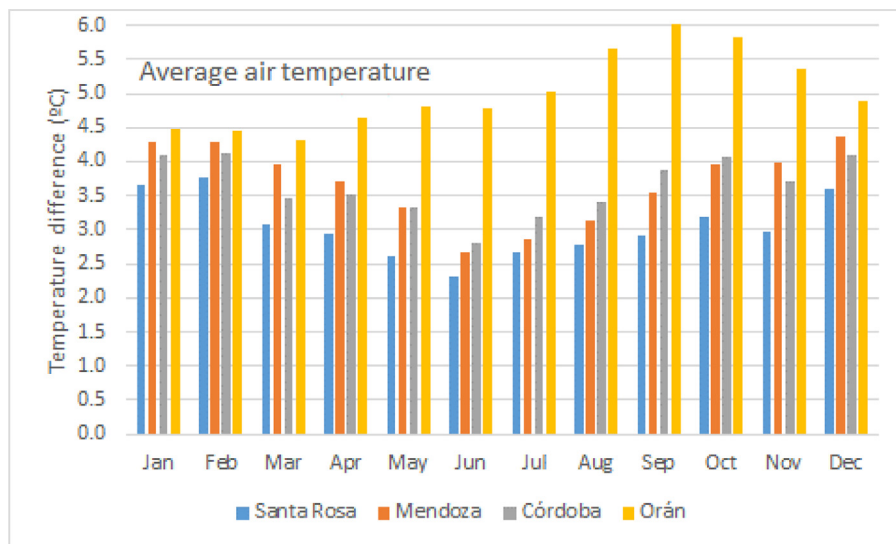


Fig. 4. Temperature difference of the average air temperature, between monthly average in 2080 and monthly average in the period 1961–1990, for the four sites.

Table 5

Annual average values of some climate parameters in the four cities for 2020, 2050 and 2080. HadCM3 model, scenario A2. TMY (1961–1990) is included as a reference.

	TMY	2020	2050	2080
<b>Santa Rosa</b>				
Dry-bulb temperature ( °C)	15.4	16.3	17.2	18.5
Solar irradiance (W/m <sup>2</sup> )	178	177	178	176
RH (%)	3.3	3.3	3.3	3.3
Wind speed (m/s)	66	66	65	66
<b>Mendoza</b>				
Dry-bulb temperature ( °C)	16.7	17.6	18.8	20.3
Solar irradiance (W/m <sup>2</sup> )	212	211	215	214
RH (%)	55	54	51	50
Wind speed (m/s)	3.3	3.3	3.3	3.4
<b>Córdoba</b>				
Dry-bulb temperature ( °C)	17.9	18.8	20.1	21.6
Solar irradiance (W/m <sup>2</sup> )	199	197	201	198
RH (%)	62	62	59	60
Wind speed (m/s)	5.5	5.5	5.6	5.7
<b>Orán</b>				
Dry-bulb temperature ( °C)	21.0	22.3	23.8	26.1
Solar irradiance (W/m <sup>2</sup> )	189	192	198	203
RH (%)	75	72	69	66
Wind speed (m/s)	5.8	5.9	6.0	6.2

4.3 and 6.0 °C in the average air temperature, and between 5.0 and 7.0 °C in the maximum (average) air temperature. The global model HadCM3 predicts that the highest increases will occur in spring. So, if nowadays the absolute temperature in Orán exceeds 41 °C, in 2080 hourly air temperatures of 45–47 °C can be expected, so it is a critical site with extreme overheating. For the other sites, the air average temperatures will increase between 2.3 and 4.3 °C and the maximum temperatures between 2.2 °C and 4.7 °C. Fig. 6 shows that also the minimum air temperatures will increase, so warmer nights are expected in winter and summer. In cities such as Orán, night ventilation could not be an efficient strategy in summer and thermal simulation is needed to confirm this situation.

A comparison with the monthly predictions of the HadCM3 global model with regional models shows a good agreement. Núñez et al. and Cabré et al. [37,7] used the regional model MM5 (Fifth-generation Pennsylvania-State University-NCAR non-hydrostatic mesoscale Model MM5 version 3.6) nested within the

HadAM3H model (A2 scenario) to simulate the climate change for the period 2081–2090 with baseline reference 1981–1990 and grid interval of 50 km. The authors divided the country into five sub-regions: sub-tropical, Andes, central, Patagonia and South-eastern South America, and analyzed the predictions of the regional model averaged in each region. The results for the average air temperature showed a particularly large warming in northeastern Argentina with peaks in spring (September) with local values of about 6.0 °C, in agreement with the predictions of Figs. 5–7 for Orán. The authors also found warming of about 2.5 °C in southern Argentina and Chile, for the A2 scenario. For the central region, that includes Córdoba and Santa Rosa, the highest overheating period will occur in summer (December) with differences of about 4.0 °C. This value also agrees with the predictions of Fig. 5. The Andes region is more difficult to analyze because the results of Núñez et al. [37] are averaged in a large extent in latitude (from –15°S to –38°S). Thus, in the Andes region, that includes Mendoza, the temperature change predicted by the regional model is about 3.0 °C, with a maximum in June of about 3.8 °C. Fig. 5 predicts differences between 2.7 °C (June) and 4.3 °C (December) in the average air temperature of Mendoza for 2080. Thus, it is concluded that the results of the HadCM3 global model for the four selected sites are reasonable and they can be used to simulate the hourly future behavior of the selected cities.

Two months were selected as representative of summer (January) and winter (July). The minimum, maximum and average temperatures predicted for these months, in the four sites, for years 2020, 2050 and 2080, are shown in Fig. 7. In summer 2080, Orán and Mendoza are the most affected sites: mean air temperatures of 29.5 and 30.5 °C, and maximum air temperatures exceeding 36 °C. For a more near future, in 2050, maximum temperatures in the four cities will exceed 32 °C in summer. This situation implies a significant increase in cooling loads and in energy consumption for air cooling. In winter, the increase of air temperatures for all the sites indicates that energy consumption for heating will decrease. Table 6 shows the neutrality temperatures  $T_n$  calculated from two models: ASHRAE 55–17 model (for mean outdoor temperatures falling between 10 °C and 33.5 °C) and the model of Pérez-Fargallo et al. [30] (for mean outdoor temperatures between 6.5 °C and 10 °C). Also, the limits of the comfort zones ( $T_n \pm 2.5$  °C for thermal acceptability of 90%) are shown for years 2020 and 2050. All cities will experiment a displacement of the comfort zone to higher temperatures, and the neutrality temper-

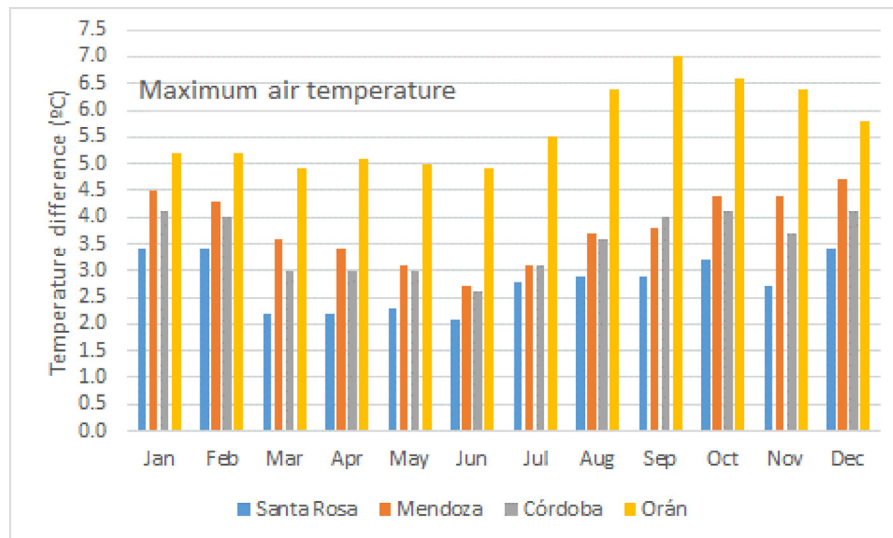


Fig. 5. Temperature difference of the maximum air temperature, between monthly average in 2080 and monthly average in the period 1961–1990, for the four sites.

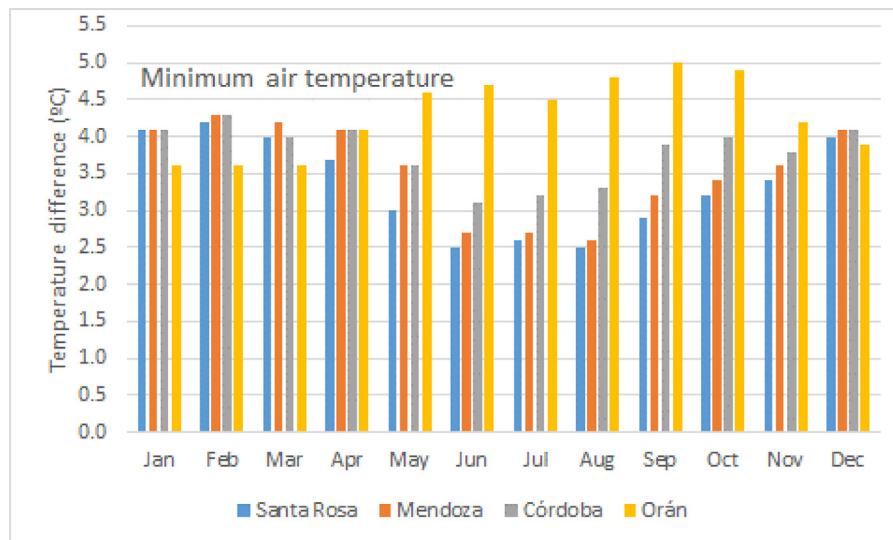


Fig. 6. Temperature difference of the minimum air temperature, between monthly average in 2080 and monthly average in the period 1961–1990, for the four sites.

Table 6

Temperature of thermal neutrality ( $T_n = 17.8^\circ\text{C} + 0.31\text{Tm}$  for  $10^\circ\text{C} < \text{Tm} < 33.5^\circ\text{C}$ ;  $T_n = 13.6^\circ\text{C} + 0.678\text{Tm}$  for  $6.5^\circ\text{C} < \text{Tm} < 10^\circ\text{C}$ ) and adaptive comfort zone for July and January (thermal acceptability of 90%), in the four studied cities, for the years 2020, 2050, and 2080.

	2020				2050				2080			
	Thermal neutrality (°C)		Comfort Zone $T_n \pm 2.5^\circ\text{C}$		Thermal neutrality (°C)		Comfort Zone $T_n \pm 2.5^\circ\text{C}$		Thermal neutrality (°C)		Comfort Zone $T_n \pm 2.5^\circ\text{C}$	
	Jul	Jan	Jul Min/Max	Jan Min/Max	Jul	Jan	Jul Min/Max	Jan Min/Max	Jul	Jan	Jul Min/Max	Jan Min/Max
Sta. Rosa	19.4	25.5	16.9/21.9	23.0/28.0	19.8	26.0	17.4/22.4	23.5/28.5	21.0	26.3	18.5/23.5	23.8/28.8
Mendoza	19.4	26.0	16.9/21.9	23.5/28.5	19.9	26.5	17.4/22.4	24.0/29.0	21.0	26.9	18.5/23.5	24.4/29.4
Córdoba	21.6	25.6	19.1/24.1	23.1/28.1	21.9	26.1	19.4/24.4	23.6/28.6	22.3	26.6	19.8/24.8	24.1/29.1
Orán	22.5	26.2	20.0/25.0	23.7/28.7	23.0	26.7	20.5/25.5	24.2/29.2	23.7	27.3	21.2/26.2	24.8/29.8

atures in summer will increase from  $25.2^\circ\text{C}$ – $25.9^\circ\text{C}$  in the baseline period to values between  $26.3$  and  $27.3^\circ\text{C}$  in 2080. This implies an average increase of the neutrality temperature of about  $1.2^\circ\text{C}$  between the baseline period (1961–1990) and 2080. For example, in Santa Rosa, the neutrality temperature in summer will move from  $25.2^\circ\text{C}$  to  $26.3^\circ\text{C}$  in 2080. In Orán, the neutrality temperature  $T_n$  of  $25.9^\circ\text{C}$  will move up to  $27.3^\circ\text{C}$  in January 2080, with limits of the comfort zone ( $T_n \pm 2.5^\circ\text{C}$ ) between  $24.8^\circ\text{C}$  and  $29.8^\circ\text{C}$ .

#### 4.2. Energy consumption for the case-study building

The results of the annual energy consumption (air heating and cooling) of the case study simulated with EnergyPlus for the years 2020, 2050 and 2080 in the four sites are shown in Table 7. When total energy consumption for heating and cooling for 2080 is compared with the baseline period 1961–1990, reductions of 16% (Santa Rosa), 8% (Mendoza), and 25% (Córdoba) are obtained; while in Orán, an increase of about 6% is observed. The energy destined

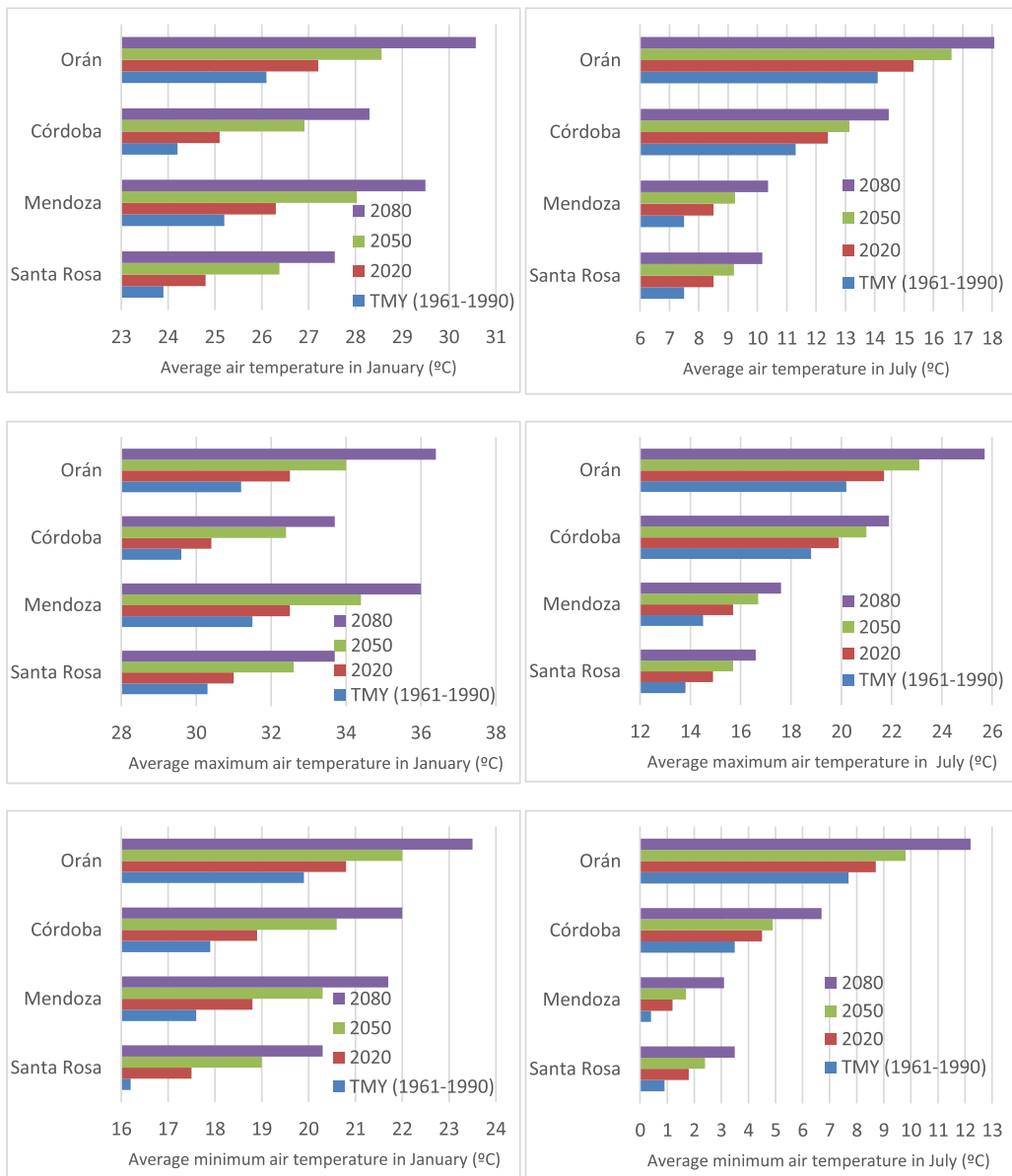


Fig. 7. Mean, maximum and minimum air temperatures for January (left) and July (right), for years 2020, 2050 and 2080. TMY is also shown as a reference.

Table 7

Annual energy consumption (air heating and cooling, in kWh) of the case study simulated with EnergyPlus for the baseline period (1961–1990) and for 2080 in the four sites, increase/decrease in energy consumption per square meter and per decade. Also, relative participation of heating/cooling in the total annual consumption is shown.

		S. Rosa	Mendoza	Córdoba	Orán
Heating energy	TMY (kWh)	12,150	9154	9117	5779
	2080 (kWh)	9339	6456	5727	2373
	ΔE (kWh/m <sup>2</sup> -decade)	−6.2	−6.0	−7.5	−7.6
Cooling energy	TMY (kWh)	295	564	149	968
	2080 (kWh)	1053	2498	1182	4764
	ΔE (kWh/m <sup>2</sup> -decade)	1.7	4.3	2.3	8.4
Annual energy	TMY (kWh)	12,445	9718	9266	6747
	2080 (kWh)	10,392	8954	6909	7137
	ΔE (kWh/m <sup>2</sup> -decade)	−4.6	−1.7	−5.2	0.9
% of Annual	Destined for heating (TMY)	98	94	98	86
	Destined to cooling (TMY)	2	6	2	14
	Destined for heating (2080)	90	72	83	33
	Destined to cooling (2080)	10	28	17	67

**Table 8**

Statistical results of the linear correlation between monthly energy consumption and monthly mean outdoor temperature in January (summer) and July (winter), for TMY, 2020, 2050 and 2080.

		R2 (%)	Correlation coefficient	P-value
January	Santa Rosa	99.5	0.998	0.0023
	Mendoza	99.9	0.999	0.0004
	Córdoba	99.3	0.996	0.0037
	Orán	99.9	0.999	0.0001
July	Santa Rosa	97.2	-0.985	0.014
	Mendoza	96.8	-0.984	0.0161
	Córdoba	94.7	-0.973	0.0269
	Orán	98.4	-0.992	0.0079

to air heating in 2080 is 23% (Santa Rosa), 29% (Mendoza), 37% (Córdoba) and 59% (Orán) lower than the consumption for air heating in the baseline period (1961–1990). On the opposite, an important increase in the consumption for air cooling is observed: 3.6 times the baseline consumption in Santa Rosa, 4.4 times in Mendoza, 7.9 in Córdoba, and 4.9 times in Orán. Because consumption for heating will be reduced in all cities, this means that the heating needs will decrease more than the increase in the cooling needs. That is, a lower relative participation of heating energy in the total consumption will be observed in all sites. From Table 7, the estimation of the increase/decrease in energy consumption per decade and square meter shows that a decrease between 6.0 and 7.6 kWh/m<sup>2</sup>-decade is observed for heating, while an increase between 1.7 and 8.4 kWh/m<sup>2</sup>-decade is observed for cooling. In a complete year, annual energy consumption will decrease between 1.7 and 4.6 kWh/m<sup>2</sup>-decade in Santa Rosa, Mendoza, and Córdoba. In the northern Orán, it will increase by about 0.9 kWh/m<sup>2</sup>-decade.

Fig. 8 shows the monthly energy consumption from TMY to 2080, for the four sites. The maximum monthly energy consumption for heating corresponds to July, while the maximum consumption for cooling corresponds to January. As expected, the coldest site (Santa Rosa), presents the highest winter consumption and the warmest one (Orán) presents the higher summer energy consumption. Again, January and July were selected for a deeper statistical analysis, shown in Table 8. In each site, a linear relationship was found between the monthly energy consumption for cooling in summer and the monthly mean outdoor temperature, with R<sup>2</sup> values higher than 99%, correlation coefficients higher than 0.99 and P-values lower than 0.0037, thus indicating a strong and positive correlation between variables with a confidence level of 95%. The same linear relationship, statistically significant, was also found in winter (R<sup>2</sup> higher than 94.7, correlation coefficients of -0.97 and P-values lower than 0.0269), with negative correlation coefficients indicating that higher minimum temperatures produce lower energy consumptions in winter.

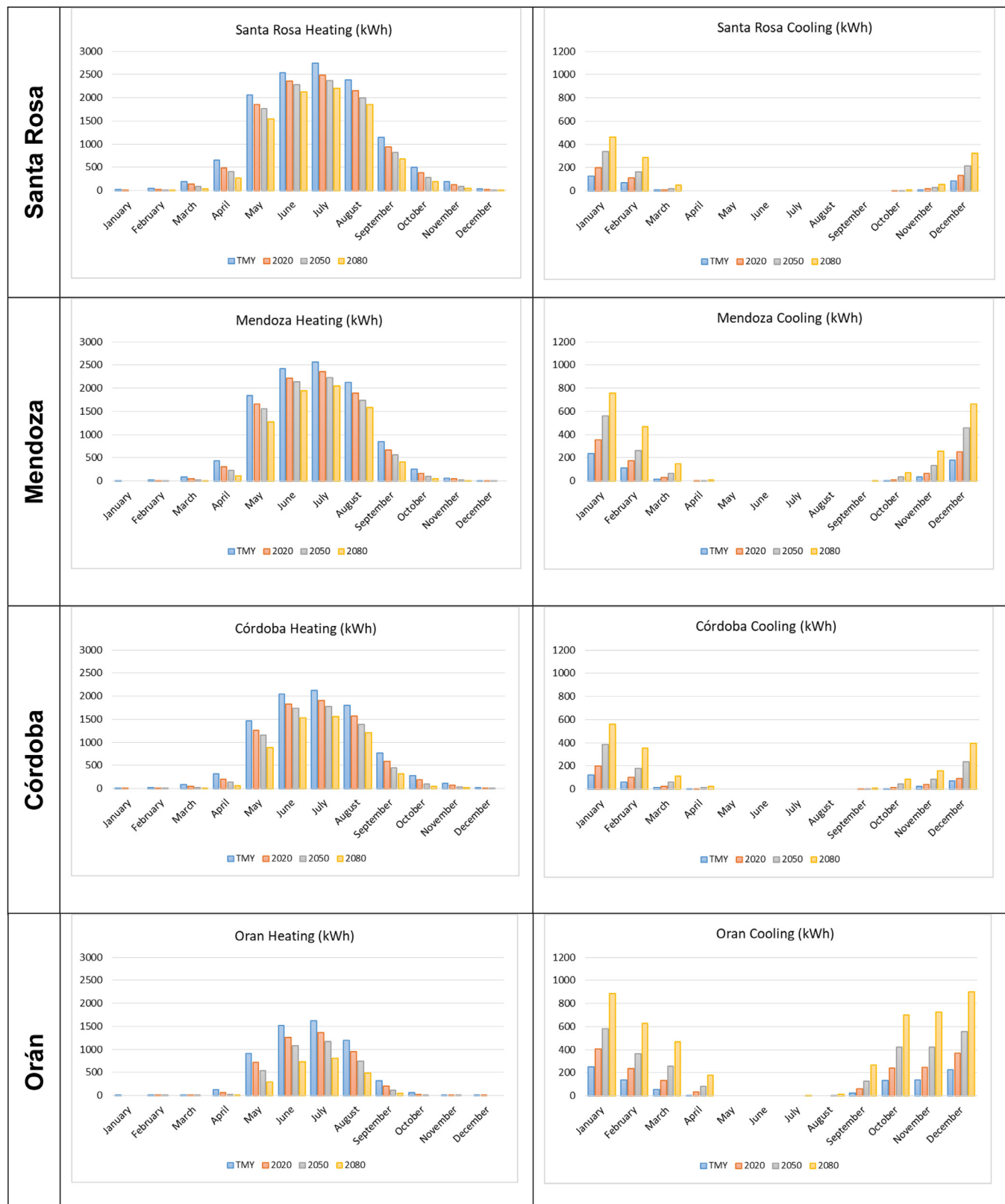
Fig. 9 shows the linear relationship between energy consumption and outdoor air temperature both, in winter and summer, for the four sites. In these graphs, energy consumption for each period (TMY, 2020, 2050 and 2080) was plotted against the predicted monthly mean maximum/minimum for each site. It is interesting to note that, independently of the different climatic conditions of the sites, a linear relationship is obtained. Thus, for each 1 °C of increment in monthly mean outdoor temperature in summer (January), an increase of about 2.2 kWh/m<sup>2</sup> is predicted. Similarly, for each 1 °C of increment in monthly mean outdoor temperature in winter (July), a decrease of 3.0 kWh/m<sup>2</sup> is predicted. These values allow roughly estimating the increase of energy consumption at the urban scale. In Santa Rosa, where 3.4 °C of mean air temperature increment is expected in January 2080 due to the climate change, an increase of about 6.2 MWh (56,575 users) is estimated, representing about 3% of the imported energy in this city.

Finally, Fig. 10 shows the annual energy consumption per square meter versus the annual mean temperature calculated for the four periods (TMY, 2020, 2050 and 2080) and for each site. Here, it is interesting to note that Santa Rosa, Mendoza, and Córdoba presents a decreasing tendency with time: total energy consumption will decrease in the future. The reason is that the three cities have a high relative participation of heating in the annual energy consumption, so higher winter temperatures in the future will cause the reduction of energy consumption for heating. On the opposite, Orán has a different (parabolic) behavior: up to 2020 the annual energy consumption will decrease, but since 2050 to the future, the cooling needs will exceed the heating needs and energy consumption will rise. It can be concluded that the impact of climate change depends on the region and climate: in temperate climates the annual consumption will decrease, but in hot climates it will decrease down to a minimum in 2020 with an increase in the future (slower between 2020 and 2050, and more evident between 2050 and 2080).

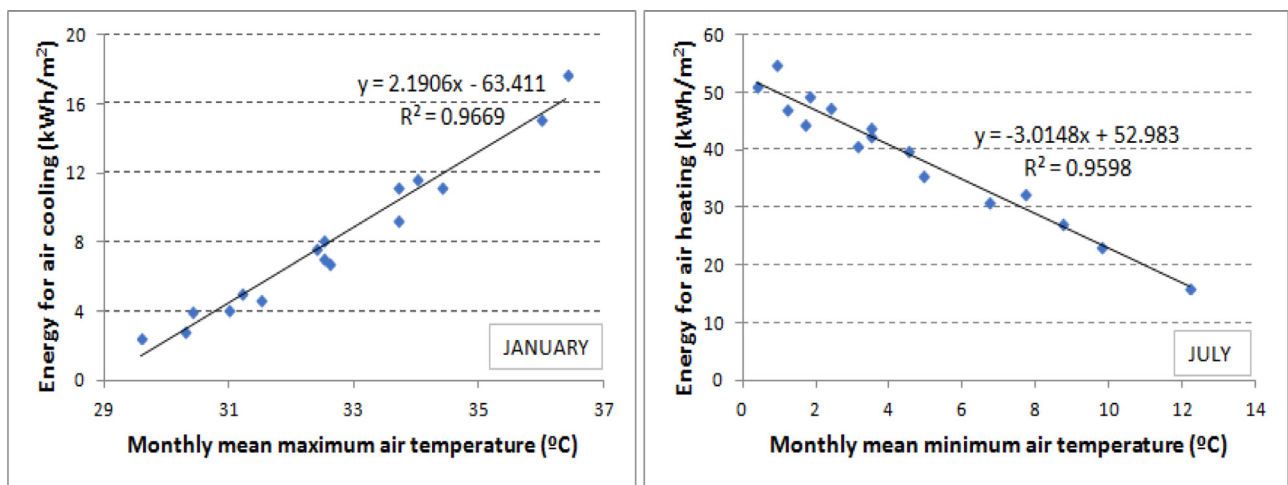
#### 4.3. Analysis of design strategies. Recommendations for building design in the future

Fig. 11 shows the percentage of hours in a month when design passive strategies can be applied, as suggested by Climate Consultant software, for the baseline period (1961–1990), and 2080. January and July were selected as representative months of summer and winter, respectively. In summer, the percentage of hours in thermal comfort will decrease from about 20% down to 10%. All sites show an increment in the hours when sun shading is needed (even in winter). Natural ventilation strategy will remain almost constant in Santa Rosa and Córdoba, but it will become less efficient in Mendoza and Orán, due to a decrease of the hours when this strategy could be effective (i.e., for Orán 28% of hours in TMY decrease to 18% in 2080). It is worthy to be noted that the efficiency of natural ventilation for a given climate depends on the air temperature and also on the wind speed. Because wind speed is not modeled by CCWorldWeatherGen tool, the decrease in efficiency shown in Fig. 11 of natural ventilation represents only to the air temperature changes. The use of thermal mass that is cooled during the night is useful at present in all sites except Orán, but in the future, it will be less efficient because of the increase in minimum air temperatures in summer. On the opposite, in winter the percentage of hours in thermal comfort will increase in the future due to the increment of outdoor air temperature in all sites. In Santa Rosa, Mendoza, and Córdoba, internal heat gains will increase their capacity of providing thermal comfort. On the contrary, in Orán the percentage of hours when internal heat gains provide thermal comfort will decrease because they could cause overheating. The same situation occurs with the direct solar gains: about 16–20% of the hours in Santa Rosa, Mendoza and Córdoba is needed, but in Orán direct solar gains will be less needed in the future.

From this analysis, it is concluded that some passive strategies that can be applied today will be less efficient in the future. Orán is the most affected city in relation to the possible passive strategies that can be applied in the design of buildings. In this city, which is representative of the north and northeast zones of Argentina with hot and humid summers, the use of direct solar gains in winter will probably cause overheating of indoor spaces, so in the future, it should be avoided. Sunshading of the building envelope (including roof and walls) is of uppermost importance, together with a highly insulated light envelope. The collection of diffuse solar gains through glazed areas should be used with caution, only for daylighting. Natural ventilation will be useful during spring and autumn, but it will be less used in summer. In this site, the use of evaporative cooling is not efficient. Some hybrid tech-



**Fig. 8.** Monthly energy consumption for TMY, 2020, 2050 and 2080 in the four sites, for the case-study.



**Fig. 9.** Energy consumption for air cooling versus monthly mean maximum outdoor air temperature in summer (January, left) and energy consumption for air heating versus monthly mean minimum outdoor air temperature in winter (July, right), per square meter, for the case-study building in the four cities and for the four periods (TMY, 2020, 2050 and 2080).

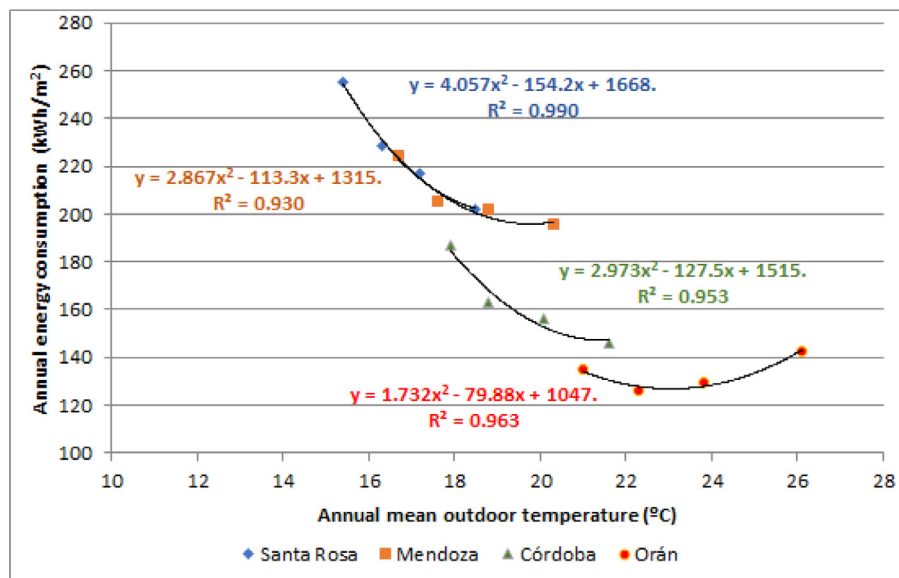


**Fig. 10.** Annual energy consumption per square meter versus annual mean temperature, for the four periods (TMY, 2020, 2050 and 2080) and for each site.

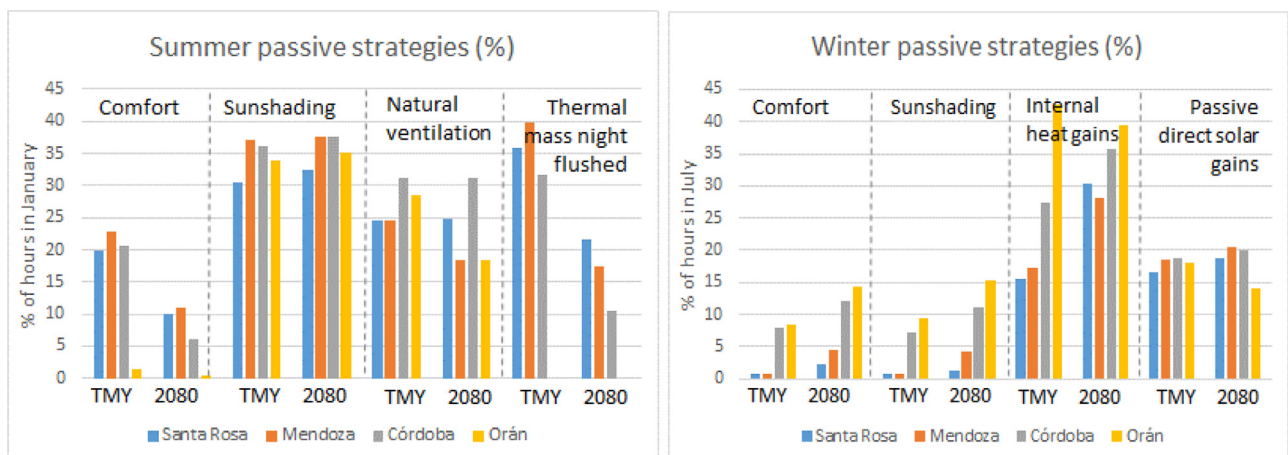


**Fig. 11.** Percentage of hours in a month when design passive strategies can be used, for the four sites, in TMY (1961–1990) and in 2080.

niques such as buried ducts with heat exchangers are more adequate.

## 5. Conclusions

Climate change will affect Argentinean regions in different ways. A set of four sites in different temperate and warm climates of Argentina were selected and the impact on energy consumption of different bioclimatic and passive strategies applied to a conventional dwelling was analyzed, for medium and long-term climate change (2020, 2050, and 2080) under A2 scenario and global model HadCM3. The four selected sites analyzed in this article are localized at different latitudes, with a maximum distance of about 1600 km between the uppermost northern site (Orán) and the bottom site (Santa Rosa). In all sites, the air temperature will increase in the future both, in winter and summer (between 2.2 °C and 3.8 °C in annual averages, with higher increases at lower latitudes). Thus, significant increases in cooling loads (3.6–7.9 times higher) and decreases in heating loads (23–59% lower) are expected in the future (2080) as compared with baseline period (1961–1990) consumption. Total annual energy consumption will decrease by 16% (Santa Rosa), 8% (Mendoza), and 25% (Córdoba) and it will increase by 6% in Orán. The obtained results obtained are limited to residential houses with similar typologies and materials of the case-study and they may not be representative at the urban scale, where the mix of different typologies, materials, and building' uses involves the use of more complex approaches.

A linear relationship between energy consumption and mean outdoor air extreme temperature both, in winter and summer and for the four sites was found. Thus, for each 1 °C of increment in monthly mean outdoor temperature in summer (January), an increase of about 2.2 kWh/m<sup>2</sup> per month is predicted. Similarly, for each 1 °C of increment in monthly mean outdoor temperature in winter (July), a decrease of 3.0 kWh/m<sup>2</sup> per month is predicted. A lower relative participation of heating energy in the total consumption will be observed in all sites.

In summer, the passive strategies analyzed through the bioclimatic chart indicate that sun shading will be needed in the future in all sites. The use of direct solar gains in winter will probably cause overheating of indoor spaces in summer, so they should be carefully designed. Passive strategies for heating could cause overheating in summer. Particular attention must be paid to cooling strategies. Natural ventilation must be analyzed from the climatic conditions of the selected site: it can be useful during spring and autumn, but less efficient in summer. The milder conditions in winter can benefit the use of renewable energies such as photovoltaic or solar, in replacement of conventional energy.

In a changing climate, it becomes absolutely necessary a regional and localized analysis of the climate and of the passive strategies in the design of buildings. The regions are differently affected by global climate change, depending on local factors such as orography, mountains, and big water reservoirs. It is very usual in Argentina that a given prototype of social housing is built by the government along the country extension, without considering regional climates. If even at present it is not adequate nor possible to generalize a prototype design to be replicated in different regions of the country, in the future this inadequacy will be more evident and the thermal comfort and energy consumption will be highly awkward. Furthermore, the demand of electricity for cooling will increase in the future and it will exert a greater pressure for the future grid, so this issue should be included in the political discussions of current and future energy investments.

## Declarations of interest

None.

## Acknowledgments

This work was supported by National Agency of Scientific and Technical Promotion (ANPCYT PICT 2014–2605) and Universidad Nacional de Salta.

## References

- [1] IEA, CO2 Emissions from Fuel Combustion. Beyond 2020 Online Database, International Energy Agency, Paris, 2012, p. 135. Available at: <http://data.iea.org>.
- [2] P. Shen, Impacts of climate change on U.S. building energy use by using down-scaled hourly future weather data, *Energy Build.* 134 (2017) 61–70.
- [3] Climate Change 2014: Mitigation of Climate Change: Working Group III Contribution to the IPCC Fifth Assessment Report, Chapter 9, Cambridge University Press, Cambridge, 2015, p. 675, doi:10.1017/CBO9781107415416.
- [4] O. Lucon, D. Urge-Vorsatz, A. Zain Ahmed, H. Akbari, P. Bertoldi, L.F. Cabeza, N. Eyre, A. Gadgil, L.D.D. Harvey, Y. Jiang, E. Liphoto, S. Mirasgedis, S. Murakami, J. Parikh, C. Pyke, M.V. Vilarino, Buildings, *Climate Change 2014: Mitigation of Climate Change, Contribution of Working Group III to the Fifth Assessment Report of the Intergovernmental Panel on Climate Change*, 2014.
- [5] WMO Statement on the State of the Global Climate in 2017, Provisional Release November 2017.
- [6] J.H. Christensen, K. Krishna Kumar, E. Aldrian, S.-I. An, I.F.A. Cavalcanti, M. de Castro, W. Dong, P. Goswami, A. Hall, J.K. Kanyanga, A. Kitoh, J. Kossin, N.-C. Lau, J. Renwick, D.B. Stephenson, S.-P. Xie, T. Zhou, Climate Phenomena and their Relevance for Future Regional Climate Change, in: T.F. Stocker, D. Qin, G.-K. Plattner, M. Tignor, S.K. Allen, J. Boschung (Eds.), *Climate Change 2013: The Physical Science Basis. Contribution of Working Group I to the Fifth Assessment Report of the Intergovernmental Panel On Climate Change*, Cambridge University Press, Cambridge, United Kingdom and New York, NY, USA, 2013.
- [7] M.F. Cabré, S. Solman, M. Núñez, Regional climate change scenarios over southern South America for future climate (2080–2099) using the MM5 Model. Mean, interannual variability and uncertainties, *Atmósfera* 29 (1) (2016) 35–60.
- [8] SMN, National Meteorological Service of Argentina, 2018. <https://www.smn.gob.ar/caracterizacion-estadisticas-de-largo-plazo>.
- [9] J. Kapsomenakis, D. Kolokotsa, T. Nikolaou, M. Santamouris, S.C. Zerefos, Forty years increase of the air ambient temperature in Greece: the impact on buildings, *Energy Convers. Manage.* 74 (2013) 353–365. <http://dx.doi.org/10.1016/j.enconman.2013.05.005>.
- [10] D.A. Assimakopoulos, M. Santamouris, I. Farrou, M. Laskari, M. Saliari, G. Zanis, G. Giannakidis, K. Tigas, J. Kapsomenakis, C. Douvis, S.C. Zerefos, T. Antonakaki, C. Giannopoulos, Modelling the energy demand projection of the building sector in Greece in the 21st century, *Energy Build.* 49 (2012) 488–498.
- [11] I. Andric, André Pina, Paulo Ferrão, Jérémie Fournier, Bruno Lacarrière, Olivier Le Corre, The impact of climate change on building heat demand in different climate types, *Energy Build.* 149 (2017) 225–234.
- [12] M. Kolokotroni, Y. Zhang, R. Watkins, London's urban heat island: impact on current and future energy consumption in office buildings, *Energy Build.* 47 (2012) 302–311.
- [13] H. Wang, Q. Chen, Impact of climate change heating and cooling energy use in buildings in the United Sates, *Energy Build.* 82 (2014) 428–436.
- [14] L. Wang, X. Liu, H. Brown, Prediction of the impacts of climate change on energy consumption for a medium-size office building with two climate models, *Energy Build.* 157 (2017) 218–226. <https://doi.org/10.1016/j.enbuild.2017.01.007>.
- [15] C. Filippín, F. Ricard, S. Flores Larsen, M. Santamouris, Retrospective analysis of the energy consumption of single-family dwellings in central Argentina. Retrofitting and adaptation to the climate change, *Renewable Energy* 101 (2017) 1226–1241.
- [16] M. Santamouris, D. Kolokotsa, Passive cooling dissipation techniques for buildings and other structures: the state of the art, *Energy Build.* 57 (2013) 74–94.
- [17] T. Karlessi, M. Santamouris, A. Synnefa, D. Assimakopoulos, P. Didaskalopoulos, K. Apostolakis, Development and testing of PCM doped cool colored coatings to mitigate urban heat island and cool buildings, *Build. Environ.* 46 (2011) 570–576 <http://dx.doi.org/10.1016/j.buildenv.2010-09-003>.
- [18] EnergyPlus, United States Department of Energy, EnergyPlus Energy Simul. Software (2018). <http://www.eere.energy.gov/buildings/energyplus>.
- [19] Meteonorm, Meteonorm software, 2018. <https://www.meteonorm.com/>.
- [20] M.F. Jentsch, A.S. Bahaj, P.B. James, Climate change future proofing of buildings -Generation and assessment of building simulation weather files, *Energy Build.* 40 (12) (2008) 2148–2168.
- [21] IRAM 11603, Acondicionamiento térmico de edificios, Clasificación bio-ambiental de la República Argentina (2011).
- [22] F. Rubel, Katharina Brugger, Klaus Haslinger, Ingeborg Auer, The climate of the European Alps: Shift of very high resolution Köppen-Geiger climate zones 1800–2100, *Meteorol. Z.* 26 (2) (2017) 115–125 Available at: [http://koeppen-geiger.vu-wien.ac.at/pdf/Paper\\_2017.pdf](http://koeppen-geiger.vu-wien.ac.at/pdf/Paper_2017.pdf).
- [23] L. Troup, D. Fannon, Morphing climate data to simulate building energy consumption, ASHRAE and IBPSA-USA SimBuild 2016 Building Performance Modeling Conference, 2016 August 8–12, 2016.
- [24] A. Moazami, S. Carlucci, S. Geving, Critical analysis of software tools aiming at generating future weather files with a view to their use in Building Performance Simulation, *Energy Procedia* 132 (2017) 640–645.

[25] SERG, Sustainable Energy Research Group, University of Southampton. Climate Change World Weather File Generator - CCWorldWeatherGen (2018). Retrieved Oct 2018, from <http://www.energy.soton.ac.uk/ccworldweathergen/>.

[26] H. Kikumoto, R. Ooka, Y. Arima, T. Yamanaka, (2015). Study on the future weather data considering the global and local climate change for building energy simulation. Vol. 14, pp. 404–4013.

[27] K. Adalberth, A. Almgren, E.H Petersen, Life cycle assessment of four multi-family buildings, *Int. J. Low Energy Sustainable Build.* 2 (2001) 1–21.

[28] O. Ortiz, C. Bonnet, J.C. Bruno, F. Castells, Sustainability based on LCM of residential dwellings: a case study in Catalonia, Spain, *Build. Environ.* 44 (2009) 84–94.

[29] ASHRAE Standard 55-2017, Thermal Environmental Conditions For Human Occupancy. American Society of Heating, Refrigerating and Air Conditioning Engineers, Atlanta GA, 2017.

[30] A. Pérez-Fargallo, J.A. Pulido-Arcas, C. Rubio-Bellido, M. Trebilcock, B. Piderit, S. Attia, Development of a new adaptive comfort model for low income housing in the central-south of Chile, *Energy Build.* 178 (2018) 94–106.

[31] UCLA, Climate Consultant V6.0 Software, University of California, Los Angeles, 2018 Available at: <http://www.energy-design-tools.aud.ucla.edu/climate-consultant/>.

[32] IRAM 11604, Aislamiento Térmico De edificios. Verificación de Sus Condiciones higrotérmicas. Ahorro de Energía En calefacción. Coeficiente volumétrico G de Pérdidas De Calor, Cálculo y valores límites, Buenos Aires, 2011.

[33] M.P. Mazzoco, C. Filippín, H. Sulaiman, S. Flores Larsen, Performance energética de una vivienda social en Argentina y su rehabilitación basada en simulación térmica, *Ambiente Construído*, Porto Alegre 18 (2018) 63–78 n. 4.

[34] A.D. González, A. Carlsson-Kanyama, E.S. Crivelli, S. Gortari, Residential energy use in one-family household with natural gas provision in a city of the Patagonian Andean region, *Energy Policy* 35 (2007) 2141–2150.

[35] IRAM 11507-1 (2001). Carpintería de obra - Ventanas exteriores. Requisitos básicos y clasificación. Buenos Aires.

[36] J Czajkowski, A Gómez, Introducción al diseño bioclimático y economía energética edilicia. Fundamentos y métodos. Publicación de la Editorial de la Universidad Nacional de La Plata, República Argentina (1994).

[37] M. Núñez, C. Solman, M. Cabré, Regional climate change experiments over southern South America. II: Climate change scenarios in the late twenty-first century, *Clim. Dyn.* 32 (2009) 1081–1095 Ed. Springer.